

Surface nanostructures induced by slow highly charged ions on CaF₂ single crystals

A. S. El-Said¹, W. Meissl¹, M. C. Simon¹, J. R. Crespo López-Urrutia²,
I. C. Gebeshuber¹, M. Lang³, HP. Winter¹, J. Ullrich², and F. Aumayr^{1*}

¹ Institut für Allgemeine Physik, Technische Universität Wien, A-1040 Wien, Austria

² Max-Planck Institut für Kernphysik, D-69029 Heidelberg, Germany

³ Gesellschaft für Schwerionenforschung, D-64291 Darmstadt, Germany

Abstract

We present first results on the generation of surface nanostructures by slow HCI on cleaved CaF₂ (111) surfaces. The CaF₂ single crystals were irradiated with slow ($v \ll 1$ a.u.) Xe⁴⁴⁺ HCI from the Heidelberg-EBIT. Like for other ionic fluoride single crystals, ion-induced surface structures in CaF₂ are known to be stable in atmospheric conditions at room temperature. After irradiation the crystals were investigated by scanning force microscopy. Topographic images reveal the generation of nanometric hillocks protruding from the surface. The number of hillocks per unit area is in agreement with the applied ion fluence. A discussion of the role of the potential energy as well as a comparison with observations for swift heavy ion irradiations of CaF₂ single crystals are presented.

PACS Nos. 79.20.Rf; 68.37.Ps; 68.35.Dv

* corresponding author

e-mail: aumayr@iap.tuwien.ac.at, Tel.: +43 1 58801 13430, Fax: +43 1 58801 13499

Institut f. Allgemeine Physik, TU Wien, Wiedner Haupstr. 8/E134, A-1040 Vienna, Austria

1. INTRODUCTION

Damage creation in ion-surface collisions is strongly correlated to ion-energy deposition in the solid and therefore depends on both the kinetic and the potential energies carried by the ions [1]. The kinetic energy loss of a projectile (stopping power) is usually subdivided into an "electronic" (inelastic) and a "nuclear" (elastic) part (see insert in fig. 1).

For slow singly charged or neutral atoms, nuclear stopping dominates the energy loss (case ① in fig. 1). This energy transfer to target cores leads to atomic displacements and lattice vibrations in the target (phonons) and can become sufficiently large to initiate a collision cascade where also the recoiling target atoms contribute to electronic excitation and displacement in the solid [2]. The low kinetic energy of the incident projectile limits its total path length and therefore the region where energy is deposited to a few monolayers close to the surface [3].

For swift ions or atoms (case ② in fig. 1) scattering from the target nuclei becomes negligible, but the now dominant electronic energy loss leads to a high ionization density around the (practically straight) ion tracks (see e.g. [4], [5] and refs. therein). In addition, inner shell ionization processes produce fast δ electrons which can considerably enlarge the region where electronic excitation /ionization of the target takes place.

For slow highly charged ions (HCI, case ③ in fig. 1) the potential energy (e.g. 51 keV in the case of Xe^{44+}) can be similar to or even exceed the ions kinetic energy. Via series of Auger processes, e.g., Auger neutralization, resonant capture followed by Auger de-excitation or multiple resonant capture followed by auto-ionization, the HCI potential energy is then transferred to the electronic subsystem of the solid within a shallow region close to the HCI impact zone (formation of "hollow atoms" see e.g. [6-9]), leading to a strong electronic excitation of a nanometer size surface area [2].

In recent years, great efforts have been made to investigate the surface damage induced by high energy ions (MeV to GeV impact energy region) in several ionic fluoride single crystals e.g. LiF, CaF₂, BaF₂, MgF₂, and LaF₃ [10-14]. While the long term goal of these studies was to reach a clearer understanding of the damage creation mechanisms, the short term goal aimed at obtaining information about the created surface features and their dependence on the

ion-beam parameters and material properties. Scanning force microscopy (SFM) has been used as the primary tool to observe surface structures on insulating surfaces on a nanometer scale [15]. The SFM micrographs of the swift ion-irradiated single ionic fluoride crystals showed nanoscopic hillocks protruding from the surface. However, such hillocks are only found for projectile ions where the electronic energy loss (S_e) exceeds typically a threshold of 5 keV/nm [11, 13]. Above this threshold both the diameter and height of the hillocks increase with the electronic stopping power S_e [13].

The nanostructures created by swift heavy ions are usually accompanied by damage created deep inside the bulk. This sets limits for using high-energy ions in nano-technological applications. Continuous development of ion source technology in the recent years made it possible to produce beams of slow ($v < v_{\text{Bohr}} = 2.19 \times 10^6$ m/s) highly charged ions (HCI) and use them for ion-surface interaction studies [9, 16-22].

In this report we present first results from SFM investigations of surface nanostructures induced by HCI in an ionic crystal interesting for various applications, namely calcium fluoride (CaF_2).

2. EXPERIMENTS

The experiments were performed on $\text{CaF}_2(111)$ surfaces freshly cleaved in air. Cleavage is known to result in a fluorine-terminated surface. Contact mode ambient atomic force microscopy (AFM) on this surface has been performed and revealed large atomically flat terraces with occasional cleavage steps, separating individual terraces. Several freshly cleaved samples were mounted on a special target holder and transferred into the vacuum chamber which was evacuated to a base pressure in the 10^{-10} mbar range. The $\text{CaF}_2(111)$ single crystal targets were then irradiated at room temperature with $^{129}\text{Xe}^{44+}$ ions from the Heidelberg-EBIT (electron beam ion trap) [23] using two different ion impact energies (2.2 keV/amu and 3.3 keV/amu). Typical ion fluxes of 10^4 ions/s (measured via electron emission statistics detection[24, 25]) and an irradiation time of several hours resulted in a total ion fluence of 2×10^9 ions/cm².

After irradiation, the crystals were investigated by an MFP-3D scanning force microscope (Asylum Research, Santa Barbara, US) under ambient conditions. This system is equipped with closed-loop nanopositioning system sensors for the correction of piezo hysteresis and creep. Furthermore it allows for simultaneous SFM and optical measurements of transparent and opaque samples due to top-view optics and an inverted microscope base. The measurements have been performed in contact mode at constant loading force of less than 10 nN, using non-conductive Si_3N_4 sensors (Veeco Instruments, France) with cantilevers of force constants of about 0.1 N/m.

3. RESULTS AND DISCUSSION

Fig. 2 shows examples of typical SFM topographic images of $\text{CaF}_2(111)$ after irradiation with Xe^{44+} ions of 2.2 keV/amu and 3.3 keV/amu impact energy per unit mass, respectively. Surprisingly, hillock-like nanostructures protruding from the surface are observed despite the fact that the electronic energy loss of the projectile ions in CaF_2 is well below the kinetic threshold for hillock production of 5 keV/nm (see table 1). The SFM images were evaluated with respect to hillock height and width distributions (see fig. 3) as well as hillock number. The number of hillocks per unit area was found to be in good agreement with the applied ion fluence. This means that (similar to the case of slow HCI impact on HOPG; see e.g. [19, 26]) basically each observed hillock results from an individual ion impact. The shape of the hillocks is almost circular. Due to the low surface roughness of the non-irradiated samples, the dimensional analysis was easy to perform. The diameter of the hillocks is defined by two opposite points marking the intersections of a vertical line profile through the hillock maximum with the undisturbed CaF_2 surface [13]. A slight change of the set point (loading force) did not lead to an observable change of the measured features. We are well aware of the possible occurrence of a systematic error of the order of few nanometers for the hillock diameter caused by the finite tip curvature radius. In contrast to the diameter, the height should not be affected by the finite SFM tip radius but mainly by the roughness of the sample. The mean hillocks diameter and height were determined by fitting a Gaussian function to the hillock frequency-versus-diameter /- height histograms (fig. 3). In table 1 the ion-irradiation

parameters (some of them estimated by using TRIM [3]) as well as the measured mean hillock diameters and height values are given. No significant difference in hillock size was found for the two different Xe^{44+} impact energies of 2.2 and 3.3 keV/amu. This independence on impact energy together with the fact that our experiments have been conducted for S_e values well below the kinetic threshold for hillock production leads us to the conclusion that the potential energy stored in Xe^{44+} ions (i.e. the sum of ionization potentials) of about 51 keV should be responsible for the hillock production.

Table 1 also compares the results of our measurements to the hillock dimensions observed for swift Xe ion impact from [11]. Surprisingly, the mean diameter of the hillocks in case of low energy Xe^{44+} bombardment is comparable to (even slightly larger than) the diameters observed after irradiation with Xe ions of more than 800 MeV kinetic energy, while the hillock height is about a factor of 4 smaller. The similarity between the two cases is probably a result of the fact, that both swift heavy ions and slow HCI initially transfer their energy to the electronic system of the target, leading to a region of strong electronic excitation (see fig. 1 and discussion in chapter 1).

Our results therefore not only show for the first time that nano-sized hillocks on a CaF_2 (111) surface can be produced by impact of slow HCI, but also demonstrate the relevance of the potential energy of the projectiles for creation of these nanostructures. By performing SFM investigations of the hillock size as a function of the potential of the projectile HCI (by varying the projectile charge state and species) we hope to achieve a clearer understanding of the hillock formation mechanism. Such investigations are currently in progress.

ACKNOWLEDGEMENTS

This work has been supported by Austrian Science Foundation FWF (Projects No. M894-N02 and P17449). The experiments were performed at the distributed LEIF-Infrastructure at MPI Heidelberg Germany, supported by Transnational Access granted by the European Project HPRI-CT-2005-026015.

REFERENCES

- [1] H. Gnaser, *Low-Energy Ion Irradiation of Solid Surfaces* (Springer Berlin, 1999).
- [2] *Fundamental Processes in Sputtering of Atoms and Molecules (SPUT 92)*, edited by P. Sigmund (Mat.Fys.Medd., Copenhagen, 1993).
- [3] J. F. Ziegler, J. P. Biersack, and U. Littmark, *The Stopping and Range of Ions in Matter* (Pergamon, New York, 1985).
- [4] G. Schiewietz, E. Luderer, G. Xiao, and P. L. Grande, *Nucl. Instrum. Meth. Phys. Res. B* 175, 1 (2001).
- [5] W. M. Arnoldbik, N. Tomozeiu, and F. H. P. M. Habraken, *Nucl. Instrum. Meth. Phys. Res. B* 203, 151 (2003).
- [6] A. Arnau, et al., *Surf. Sci. Reports* 27, 113 (1997).
- [7] H. P. Winter and F. Aumayr, *J. Phys. B: At. Mol. Opt. Phys.* 32, R39 (1999).
- [8] H. P. Winter and F. Aumayr, *Euro. Phys. News* 33, 215 (2002).
- [9] F. Aumayr and H. P. Winter, *Phil. Trans. Roy. Soc. (London)* 362, 77 (2004).
- [10] C. Müller, A. Benyagoub, M. Lang, R. Neumann, K. Schwartz, M. Toulemonde, and C. Trautmann, *Nucl. Instrum. Meth. Phys. Res. B* 209, 175 (2003).
- [11] C. Müller, M. Cranney, A. S. El-Said, N. Ishikawa, A. Iwase, M. Lang, and R. Neumann, *Nucl. Instrum. Meth. Phys. Res. B* 191, 246 (2002).
- [12] N. Khalfaoui, C. C. Rotaru, S. Bouffard, M. Toulemonde, J. P. Stoquert, F. Haas, C. Trautmann, J. Jensen, and A. Dunlop, *Nucl. Instrum. Meth. Phys. Res. B* 240, 819 (2005).
- [13] A. S. El-Said, M. Cranney, N. Ishikawa, A. Iwase, R. Neumann, K. Schwartz, M. Toulemonde, and C. Trautmann, *Nucl. Instrum. Meth. Phys. Res. B* 218, 492 (2004).
- [14] A. S. El-Said, R. Neumann, K. Schwartz, and C. Trautmann, *Rad. Eff. Def. Sol.* 157, 649 (2002).
- [15] G. Binning, C. F. Quate, and C. Gerber, *Phys. Rev. Lett.* 56, 930 (1986).
- [16] D. Schneider, et al., *Phys.Rev.A* 42, 3889 (1990).
- [17] T. Schenkel, A. V. Hamza, A. V. Barnes, and D. H. Schneider, *Progr. Surf. Sci.* 61, 23 (1999).

- [18] L. P. Ratliff, E. W. Bell, D. C. Parks, A. I. Pikin, and J. D. Gillaspay, *Appl. Phys. Lett.* 75, 590 (1999).
- [19] G. Hayderer, S. Cernusca, M. Schmid, P. Varga, H. Winter, and F. Aumayr, *Physica Scripta T92*, 156 (2000).
- [20] F. Aumayr and H. P. Winter, *e-J. Surf. Sci. Nanotech.* 1, 171 (2003).
- [21] N. Nakamura, M. Terada, Y. Nakai, Y. Kanai, S. Ohtani, K. Komaki, and Y. Yamazaki, *Nucl. Instrum. Meth. Phys. Res. B* 232, 261 (2005).
- [22] M. Terada, N. Nakamura, Y. Nakai, Y. Kanai, S. Ohtani, K. Komaki, and Y. Yamazaki, *Nucl. Instrum. Meth. Phys. Res. B* 235, 452 (2005).
- [23] J. R. Crespo López-Urrutia, B. Bapat, B. Feuerstein, D. Fischer, H. Lörch, R. Moshhammer, and J. Ullrich, *Hyperfine Interactions* 146/147, 109 (2003).
- [24] F. Aumayr, G. Lakits, and H. P. Winter, *Appl.Surf.Sci.* 47, 139 (1991).
- [25] W. Meissl, M. C. Simon, J. R. Crespo Lopez-Urrutia, H. Tawara, J. Ullrich, H. P. Winter, and F. Aumayr, *Rev. Sci. Instrum.*, in print (2006).
- [26] S. Takahashi, M. Tona, K. Nagata, N. Yoshiyasu, N. Nakamura, M. Sakurai, C. Yamada, and S. Ohtani, *Nucl. Instrum. Meth. Phys. Res. B* 235, 456 (2005);
N. Yoshiyasu et al., *Jpn. J. Appl. Phys.*, 45, 995-997 (2006).

TABLE 1. Ion-beam parameters and measured hillocks sizes

	Slow Xe ⁴⁴⁺	Slow Xe ⁴⁴⁺	Swift Xe [11]
Kinetic energy (keV/amu)	2.2	3.3	6400
Ion range (nm) [3]	84	117	46000
Electronic energy loss (keV/nm) [3]	1.09	1.31	19.5
Nuclear energy loss (keV/nm) [3]	2.85	2.56	0.02
Mean hillocks diameter (nm)	28.1 ± 0.4	28.3 ± 0.5	23.5 ± 0.4
Mean hillocks height (nm)	0.9 ± 0.1	0.9 ± 0.1	3.8 ± 0.2

FIGURE CAPTIONS

- Fig. 1** Energy deposition during interaction with a solid surface (schematic, c.f. text) of ① slow single charged ions or neutral atoms, ② swift ions or neutral atoms, ③ slow highly charged ions.
- Fig. 2** Topographic SFM images for CaF₂ single crystal irradiated with Xe⁴⁴⁺ ($E_k = 2.2$ keV/amu) [left] and Xe⁴⁴⁺ ($E_k = 3.3$ keV/amu) [right] ions.
- Fig. 3** Frequency distribution of hillock diameter (left) and hillock height (right) for CaF₂ single crystal irradiated with Xe⁴⁴⁺ ($E_k = 3.3$ keV/amu) ions. The mean values are obtained by fitting a Gaussian curve to the data.

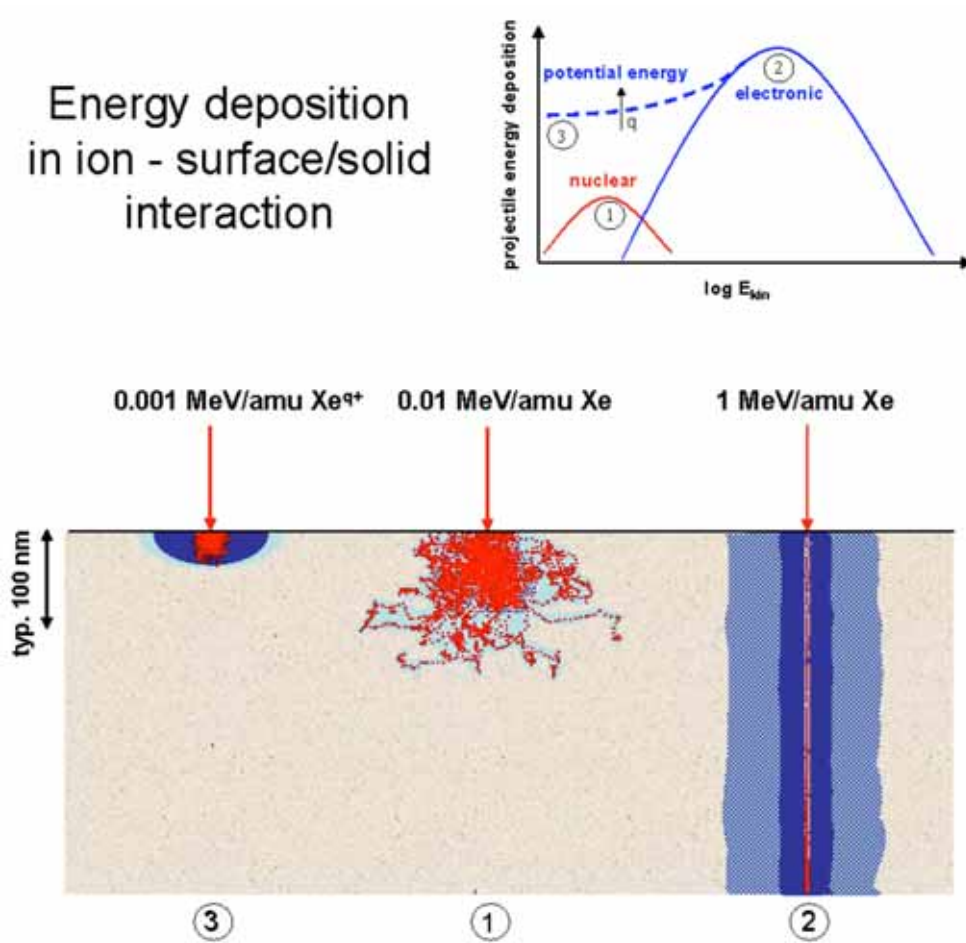
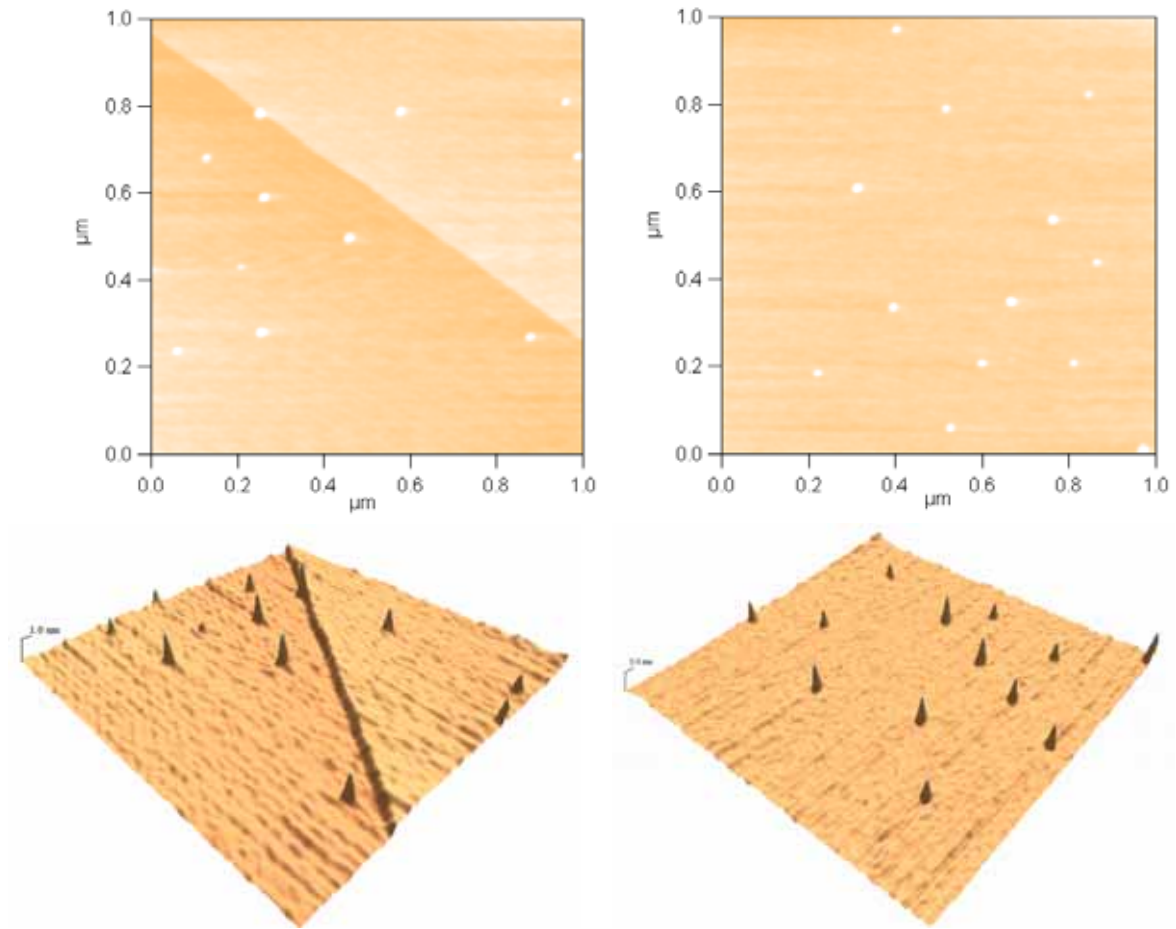


Fig. 1

**Fig. 2**

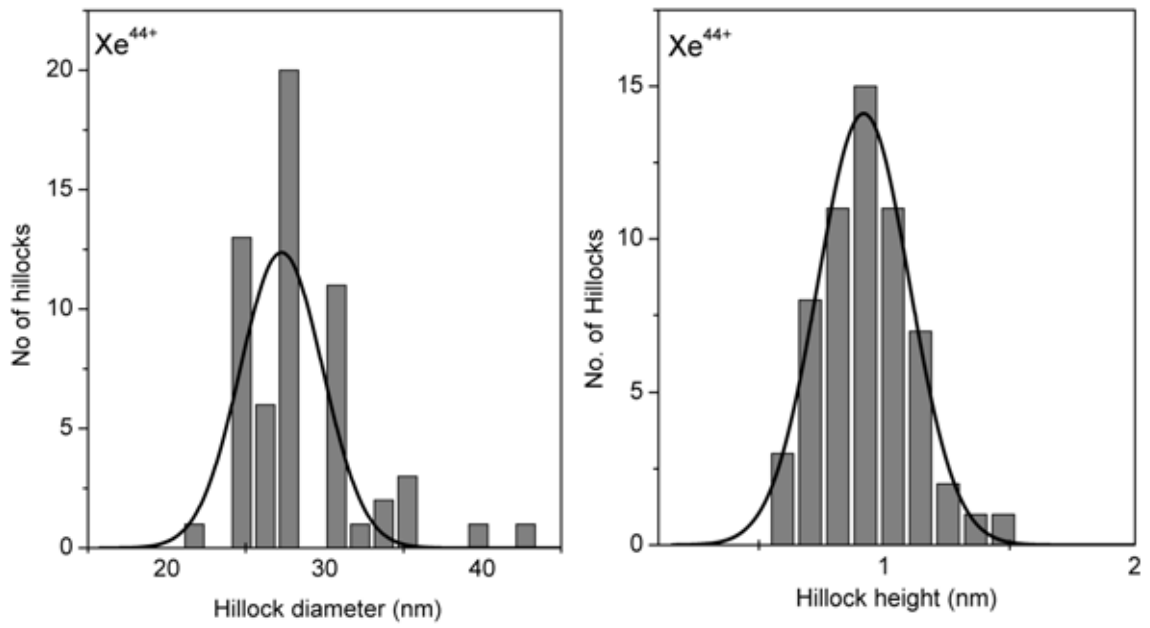


Fig. 3